On the interaction of copper with tris(hydroxymethyl)aminomethane

M. F. COLOMBO
Instituto de Biociências, Letras e Ciências Exatas – UNESP, 15.100 S. José do Rio Preto, SP, Brasil

AND

L. AUSTRILINO, O. R. NASCIMENTO, E. E. CASTELLANO, AND M. TABAK
Instituto de Física e Química de São Carlos – USP, 13.560 S. Carlos, SP, Brasil

Received July 17, 1986

M. F. COLOMBO, L. AUSTRILINO, O. R. NASCIMENTO, E. E. CASTELLANO, and M. TABAK. Can. J. Chem. **65**, 821 (1987).

The interaction of copper with tris(hydroxymethyl)aminomethane (TRIS) has been studied by optical and esr spectroscopic techniques. In solution, three different copper complexes are obtained as a function of pH. At pH 10 the room temperature esr parameters are $g_0 = 2.135$, $A_0 = 82$ G and nitrogen superhyperfine structure $A_N = 9.5$ G, characteristic of two nitrogen ligands; at pH 6.5, $g_0 = 2.147$, $A_0 = 65$ G and at pH 5.0, $g_0 = 2.180$, $A_0 = 44$ G. The high pH complex was crystallized and its molecular structure determined by X-ray methods. Space group and cell dimensions are $C2/c$, $a = 12.955(2)$ Å, $b = 10.793(1)$ Å, $c = 10.091(2)$ Å, $\beta = 116.62(1)°$, $V = 1261.4(6)$ Å^3, $Z = 4$, $D_c = 1.694$ g cm^{-3}, $R = 0.034$ for 938 reflections with $I > 3\sigma(I)$. The Cu^{2+} ion is located on the two-fold axis and coordinated to the oxygen and nitrogen atoms of two TRIS moieties; these ligand atoms form the rectangular base of a pyramid structure in which oxygen from a water molecule acts as the fifth ligand.

M. F. COLOMBO, L. AUSTRILINO, O. R. NASCIMENTO, E. E. CASTELLANO et M. TABAK. Can. J. Chem. **65**, 821 (1987).

Faisant appel à des techniques de spectroscopie optique ou rpe, on a étudié l'interaction entre le cuivre et le tris(hydroxyméthyl)aminométhane (TRIS). En solution, trois types différents de complexes de cuivre sont obtenus en fonction du pH : à un pH de 10 et à la température ambiante, les paramètres rpe sont les suivants : $g_0 = 2,135$, $A_0 = 82$ G et une structure hyperfine de l'azote $A_N = 9,5$ G qui sont caractéristiques de deux ligands azotés; à un pH de 6,5, $g_0 = 2,147$ et $A_0 = 65$ G et à un pH de 5,0, $g_0 = 2,180$ et $A_0 = 44$ G. On a cristallisé le complexe qui se forme à un pH élevé et on a déterminé sa structure par diffraction des rayons-X. Le produit cristallise dans le groupe d'espace $C2/c$, avec $a = 12,955(2)$ Å, $b = 10,793(1)$ Å et $c = 10,091(2)$ Å et $\beta = 116,62(1)°$, $V = 1261,4(6)$ Å^3, $Z = 4$, $D_c = 1,694$ g cm^{-3} et $R = 0,034$ pour 938 réflexions avec $I > 3\sigma(I)$. L'ion Cu^{2+} est situé sur l'axe binaire et il est coordonné aux atomes d'azote et d'oxygène des deux portions TRIS; les atomes de ces ligands forment la base rectangulaire d'une structure pyramidale dans laquelle l'oxygène d'une molécule d'eau agit comme cinquième ligand.

[Traduit par la revue]

Introduction

Due to the importance of the biological complexes of Cu(II) and its presence as an integral part of a number of proteins, several techniques have been used to obtain information about the binding structure and biological function of this ion. Because of the intrinsic complexity of high molecular weight systems, many model studies have been made of Cu(II) with aminoacids, small peptides and organic compounds (1).

Electron spin resonance and optical absorption spectroscopies have proved to be very useful in establishing the ligands bonded to the metallic ion, the bond symmetry and the degree of covalence in these complexes (2–4). These data are always more completely explained when the complexes formed in solution are also obtained and investigated in the solid state; in solution the copper ion often forms more than one complex for a given free ligand concentration. It is often extremely difficult to separate the complexes due to their labile character and this is why most of the work appearing in the literature is restricted to the discussion of data for samples prepared at high free ligand concentration, when the metallic ion is found as the most stable complex (5, 6).

The quantitative description and concentrations of the complexes formed in solution is made through the determination of equilibrium constants and formation curves. However, the equilibrium constants only give indirect structural information of the complexes; solid state epr and X-ray diffraction data can give a complete structural characterization (7).

In the present work the interaction of tris(hydroxymethyl)-aminomethane (TRIS) with copper is investigated with use of the epr and optical spectroscopies as well as X-ray crystallography. The choice of this compound was motivated first by its wide use as biochemical buffer and our detection of its ability to make quite strong copper complexes in competition with some biological molecules. This compound also has quite interesting properties in the solid state, where a transition is observed with the formation of a plastic crystal phase (8, 9). Further, the equilibrium constants were obtained for the Cu^{2+}—TRIS complexes in solution based on the experimental titration data and the assumption of several reaction equilibria (10). An attempt is made to characterize the complexes in solution by comparing the spectroscopic and titration data, and also to identify the complex obtained in the crystalline form by using epr and X-ray crystallography.

Experimental

Sample preparation

TRIS and $CuClO_4$ were obtained from Merck Co. and used without further purification. A solution of 0.05 *M* TRIS and 0.005 *M* $CuClO_4$ in distilled water has a characteristic blue color and the original pH value is around 8.5. The pH values in the range 3.0–12.0 (Corning Model 130 pH-meter) were adjusted with the use of concentrated solutions of NaOH and HCl so that dilution was avoided. Equal 0.5 mL aliquots at each pH value were collected from a stock of 50 mL for the measurements, and the samples were used both for electronic optical absorption and epr measurements at room temperature and at low temperature in the frozen state.

Single crystals were obtained from solutions of 1 *M* TRIS and 0.1 *M* $CuClO_4$. Generally, good crystals were obtained if the solution was maintained around pH 10.0.

Optical and esr spectroscopy

For the optical absorption measurements (350–700 nm) a spectro-

photometer Shimadzu UV-180 was used. Electron spin resonance measurements were performed in a Varian E-109 spectrometer at X-band (9.3 GHz). A rectangular cavity E-248 together with the temperature control accessory E-257 was used to obtain the spectra at room temperature and at −150°C. The signal modulation at 100 kHz was 4 G peak-to-peak and microwave power 10 mW, the power being adjusted to improve the resolution of the superhyperfine nitrogen lines. Single crystal spectra were obtained with the use of a Varian goniometer, measuring the spectra in three orthogonal crystal planes as a function of orientation of the magnetic field at room temperature.

Crystallography

A prismatic crystal with dimensions 0.52 × 0.10 × 0.10 mm was mounted on an Enraf Nonius CAD-4 diffractometer. Unit cell dimensions and the orientation matrix for data collection were obtained by least squares from 25 centered reflections. Crystal data are as follows

$Cu(TRIS)_2 \cdot H_2O$ fw = 321.81

Monoclinic, space group $C2/c$, a = 12.955(2), b = 10.793(1), c = 10.091(2) Å, β = 116.62(1)°, V = 1261.4(6) Å^3, Z = 4, D_c = 1.694 g cm^{-3}, μ(MoKα) = 1.68 mm^{-1}, λ(MoKα) = 0.71073 Å, T = 296 K.

Intensities were measured by the ω–2θ scan technique at a rate between 2.5 and 10.0° min^{-1}; the ω scan angle was (0.80 + 0.35 tan θ)°, extended at each side by 25% for background determination. From 1701 reflections measured, 1108 unique, 938 having $I > 3\sigma(I)$ ($\sigma(I)$ estimated from counting statistics) were used for structure determination and refinement. The intensity of one standard reflection ($3\bar{1}\bar{5}$) was essentially constant (variation of ±2%) over the duration of the experiment. Data were corrected for Lorentz, polarization, and absorption effects (maximum and minimum transmission factors 0.908 and 0.816).

The copper atom was readily located from a Patterson map and the rest of the structure was determined by alternate cycles of isotropic least squares and difference synthesis. The structure was refined by full-matrix least-squares, including H-atom coordinates, to final R factors R = 0.034 and R_w = 0.030. The function minimized was $\Sigma w(|F_o| - |F_c|)^2$, with $w = 1/\sigma^2(F_o)$. Hydrogen atoms were assigned a common B factor which refined to a final value of 1.2(2) Å^2. All other atoms were treated anisotropically. A total of 118 parameters were refined, including χ in the extinction correction formula $F(\text{corrected}) = F_c[1.0 - \chi F_c^2/\sin\theta]$, which converged to the value $\chi = 1.46 \times 10^{-6}$. Complex scattering factors for non-H atoms (11, 12) and bonded H-atom scattering factors (13) were employed. Most calculations were carried out with the programs SHELX-76 (14) and ORTEP (15).

Results

The formation curves for the complex in solution were calculated using the equilibrium constants and reactions proposed in the work of Bai and Martell (10). These curves predicted eight possible different complexes as a function of pH (Table 1).

Optical absorption measurements

The optical spectra for the Cu^{2+}—TRIS system as a function of pH are presented in Fig. 1. A shift of the band to lower wavelengths occurs with the increase of pH. At pH 8.1 a splitting of the absorption band into two is apparent. Figure 2 presents the dependence of the wavelength of maximum absorption of the pH. The decrease of λ with increasing pH and a splitting above pH 8.0–8.5 are clearly observed.

In order to follow the appearance of the electronic bands the intensity of absorption at two different wavelengths as a function of pH was plotted (Fig. 3). The selection of the wavelengths was made using the fact that the high pH spectrum shows two bands at approximately 630 and 530 nm. Figure 3*a* shows that the maximum intensity at 630 nm occurs at pH 7.0, while above pH 9.5 the absorption intensity remains constant.

TABLE 1. Equilibrium constants for the complexes of Cu^{2+} with TRIS in solution at 25°C, 0.10 M ionic strength (10)

Complex	Equilibrium constant	log K	pH_{max}	Maximum* concentration (%)
ML^{2+}	K_1	3.95	5.4	31
ML_2^{2+}	K_2	3.68	5.8	22
ML_3^{2+}	K_3	3.47	6.4	29
ML_4^{2+}	K_4	3.0	7.6	75
$MH_{-1}L^+$	K_{1a}	−6.0	5.9	13
$(MH_{-1}L)_2^{2+}$	K_{ad}	2.2	6.5	16
$ML(H_{-1}L)^+$	K_{2a}	−6.32	6.0	2
$M(H_{-1}L)_2$	K_{2b}	−7.90	>9	>60

*The maximum concentrations were calculated from the formation curves and are given together with the corresponding pH value.

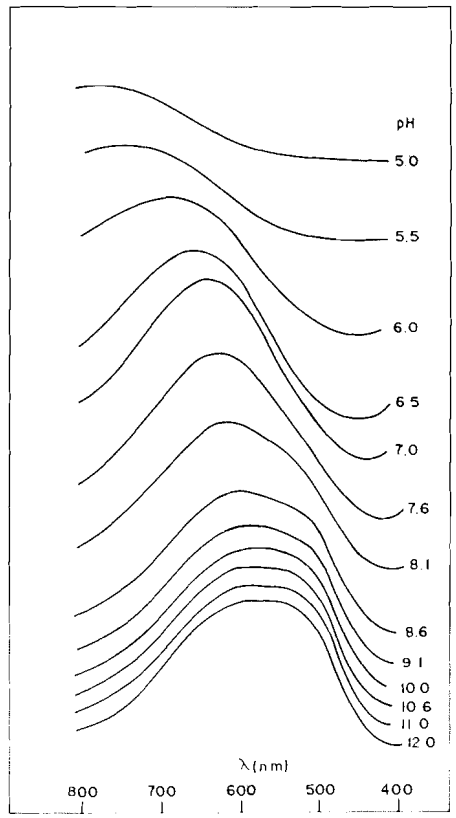

FIG. 1. Optical absorption spectra for the complexes Cu^{2+}—TRIS in solution as a function of pH.

From Fig. 3*b* the absorption at 530 nm increases with pH up to pH 9.0 and then it remains constant at approximately the intensity of the 630 nm band.

Electron spin resonance measurements

Figure 4 shows the room temperature esr spectra for the Cu^{2+}—TRIS system as a function of pH. At pH values above 8.0 a predominant spectrum is apparent with a superhyperfine splitting of the high field line into five lines probably due to two nitrogen ligands on the metal ion. From Fig. 4*b* it is evident that lowering the pH towards pH 7.0 leads to less of this complex and an increase in a second one where nitrogen structure is not resolved. This second complex has a greater value of g_0 and smaller value of A_0. We shall denote the different complexes starting from high pH so that the complex appearing above pH

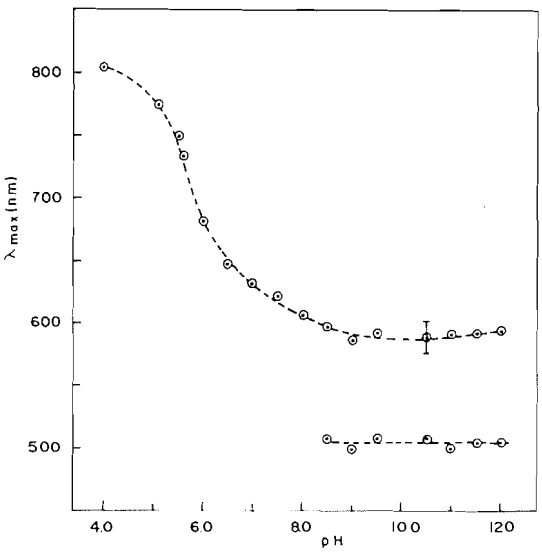

FIG. 2. Dependence of the wavelength for maximum absorption λ_{max} on the pH for the solution of Cu^{2+}—TRIS.

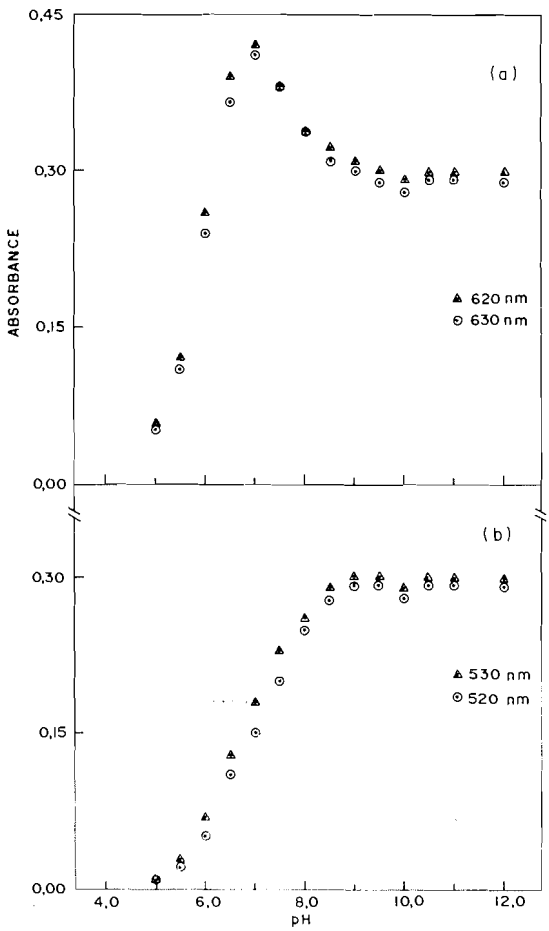

FIG. 3. Dependence of the intensity of the absorption at two different wavelengths which characterize the optical bands as a function of pH for the solution of Cu^{2+}—TRIS.

8.0 will be **1**; the second complex around pH 7.0 will be **2**, etc.

Below pH 6.5, complex **1** disappears completely and the concentration of complex **2** is reduced; in fact, the amount of this complex is reduced dramatically at pH 5.6 (Fig. 4*a*). It is clear that at pH 6.0 and specially pH 5.6 there exists a complex **2** (small amount) and another lower pH complex (**3**). Further

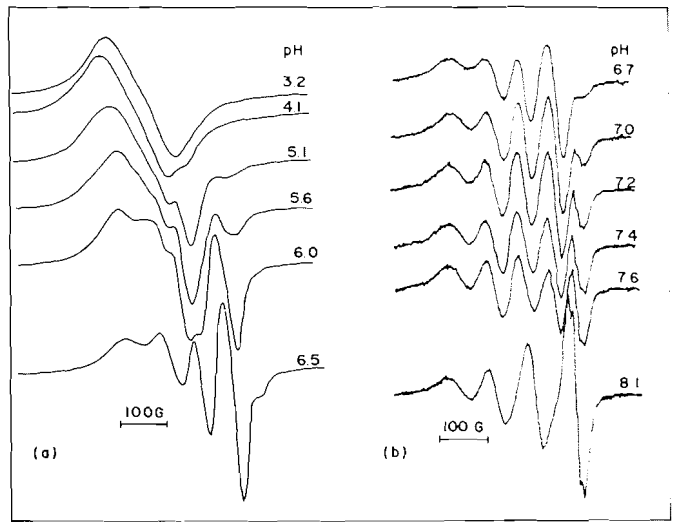

FIG. 4. Electron spin resonance spectra for the Cu^{2+}—TRIS solution as a function of pH at room temperature: (*a*) low pH range 3.2–6.5; (*b*) high pH range 6.7–8.1. Spectra above 8.1 do not change.

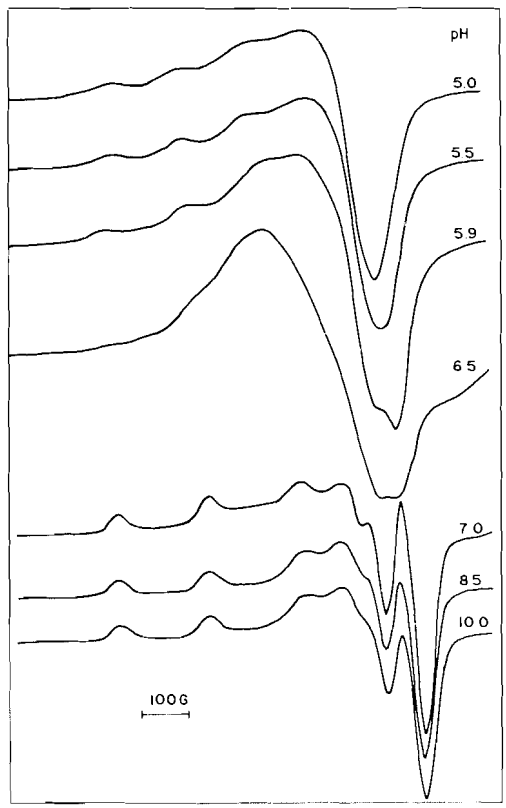

FIG. 5. Electron spin resonance spectra for the Cu^{2+}—TRIS frozen solution as a function of pH at −150°C.

lowering of pH gives the hydrated copper ion as the predominant species. In order to further characterize the observed complexes esr spectra were taken at low temperature (Fig. 5). In the pH range 7.5–12.0 the spectrum practically does not change, this being a characteristic for the high pH species. The nitrogen hyperfine structure is not resolved at this low temperature. Complex **2** starts to show up near pH 7.0 and at pH 6.5 the contribution of complex **1** is very small (Fig. 5). The very broad line with poorly resolved hyperfine structure is probably due to the fact that complex **2** is highly charged and precipitates at low temperature or, alternatively, to dimer

TABLE 2. Electron paramagnetic resonance parameters for the complexes of Cu^{2+} with TRIS in solution as a function of pH

Complex	pH	g_0	A_0 (G)	A_N (G)	λ_{max} (nm)
1	10	2.135	82	9.5	587 508
2	6.5	2.147	65	—	650
3	5.0	2.180	44	—	775
Solvated ion	3.2	2.220	—	—	~800

*The parameters correspond to those for the pure complexes obtained through spectral subtraction (complexes **2** and **3**). The wavelength for maximum absorption was also included.

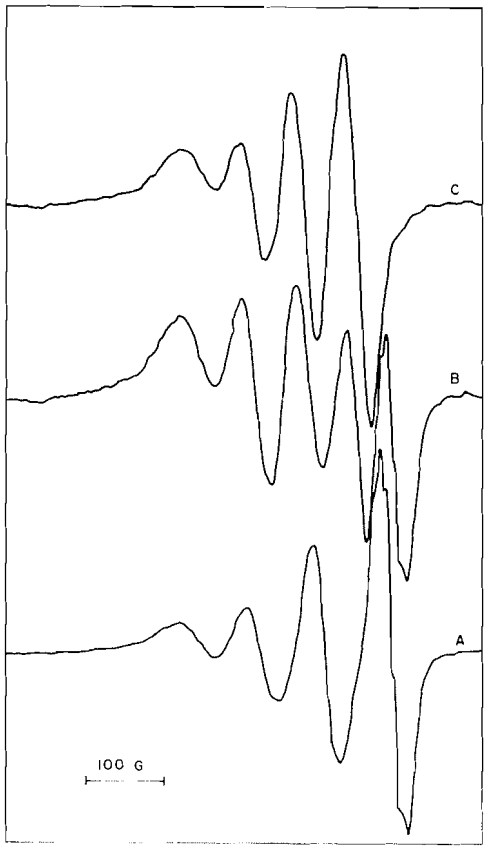

FIG. 6. Electron spin resonance spectrum for complex **2** (*C*) obtained through spectral subtraction using the experimental spectra at pH 10.0 (complex **1**, *A*) and at pH 7.6 (mixture of complexes **1** and **2**, *B*).

formation for complex **2**. It is interesting that the loss of resolution of copper hyperfine structure occurs in a very narrow pH range since both at pH 6.0 and pH 7.0 this structure again becomes resolved. The esr parameters for the complexes of Cu^{2+} with TRIS are listed in Table 2. From the spectra in Figs. 4 and 5 it is clear that the esr spectrum for **1** is pure and the parameters can be obtained with great accuracy. However, the parameters for complexes **2** and **3** can not be directly obtained due to the superposition of spectra for several complexes. To obtain the pure spectra of complexes **2** and **3**, a spectral subtraction was performed based on the relation $C = A - BX$, where *A* and *B* refer to spectra of the mixture of **1** and **2** and of pure **1**, respectively. The factor *X* is adjusted to obtain the best reproduction of the experimental spectrum (Fig. 6). The spectrum at pH 10.0 corresponds to pure complex **1** while at

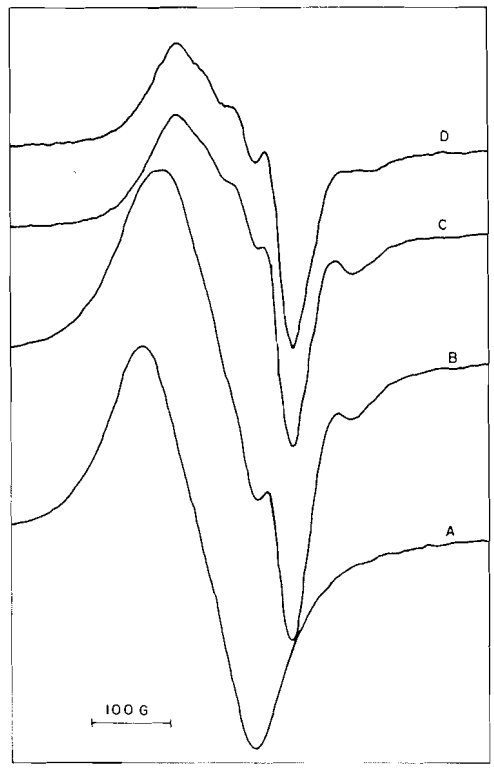

FIG. 7. Electron spin resonance spectrum for complex **3** (*D*) obtained through spectral subtraction using the experimental spectra at pH 3.2 (solvated ion *A*) and at pH 5.1 (mixture of solvated ion, complex **3** and small amount of complex **2**, *B*). The spectrum *C* was obtained from a subtraction of spectrum *A* from *B*; spectrum *D* takes in account the small amount of complex **2** in the spectrum *C*.

pH 7.6 corresponds to a contribution of both complexes. *X* turns out to be 0.45 for this case.

To obtain the spectrum of pure **3**, again the relation $C = A - BX$ was used where now *A* is the experimental spectrum at pH 5.1 and *B* is the experimental spectrum at pH 3.2, which corresponds to solvated free copper ion in solution. The result is shown in Fig. 7 ($X = 0.6$) from which it is clear that there is still a small contribution from complex **2**.

Single crystals for the high pH complex were obtained; the esr spectra and the angular variations in three orthogonal planes were measured (Fig. 8). A single esr line with no hyperfine structure is observed.

The angular variation was adjusted by the Zeeman Hamiltonian. The principal values for the g tensor are shown in Table 3. All these values are different, showing a small rhombic distortion in the symmetry of the complex.

Crystallography

Final atomic coordinates for non-hydrogen atoms and equivalent isotropic temperature factors are given in Table 4. The list of structure factors, anisotropic thermal parameters and hydrogen fractional coordinates have been deposited.[1] Bond distances and angles for the tris(hydroxymethyl)aminomethane moiety and for the coordination around the copper atom are given in Table 5.

The copper atom is located on a two-fold axis and is coordinated by an oxygen atom of a water molecule located on

[1]These tables are available from the Depository of Unpublished Data, CISTI, National Research Council of Canada, Ottawa, Ont., Canada K1A 0S2.

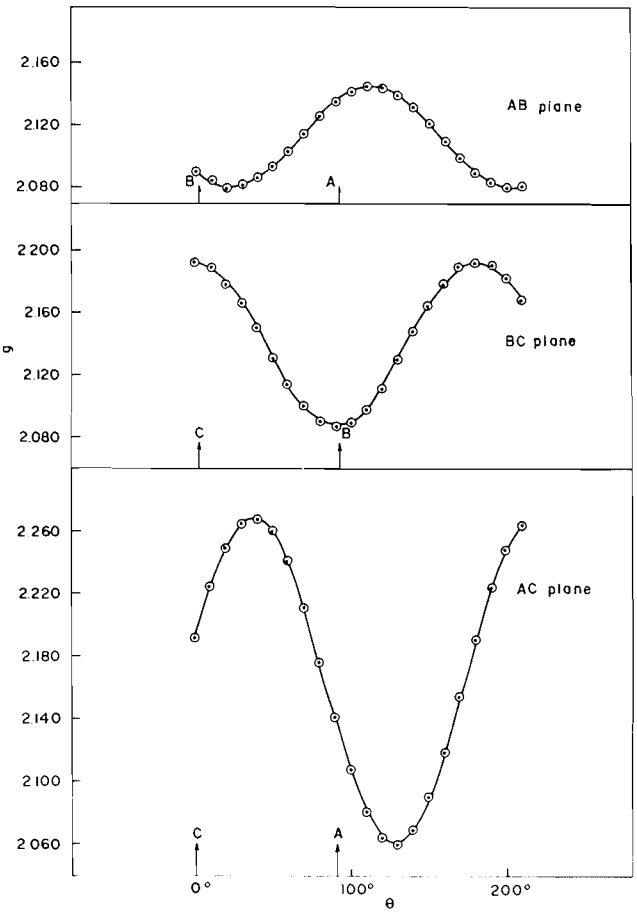

FIG. 8. Angular variations of the position of the esr spectra for the single crystal of Cu^{2+}·TRIS in three orthogonal crystal planes.

TABLE 3. Electron paramagnetic resonance parameters for the high pH complex (**1**) in solution (frozen), single crystal, and powder samples

Complex	g_1	g_2	g_3	$A_\parallel$ (G)	$A_\perp$ (G)
pH = 10 (−150°C)	2.255	2.101	2.071	190	28
Powder	2.268	2.102	2.060	—	—
Single crystal	2.268(9)	2.092(8)	2.053(6)	—	—

TABLE 4. Fractional coordinates and thermal parameters (Å^2), with standard deviations in parentheses

Atom	x/a	y/b	z/c	B_{eq}*
CU	0.0	0.2315(1)	0.25	1.63(2)
C(1)	0.1047(3)	0.2081(3)	0.0605(5)	1.8(1)
O(1)	−0.0069(2)	0.2180(2)	0.0527(3)	1.68(7)
C(2)	0.3124(3)	0.1514(4)	0.2260(5)	1.9(1)
D(2)	0.3909(2)	0.0935(2)	0.3596(3)	2.40(9)
C(3)	0.1538(3)	0.0056(3)	0.2012(5)	1.8(1)
O(3)	0.1698(2)	−0.0611(3)	0.0912(3)	2.40(9)
C(4)	0.1879(3)	0.1414(3)	0.2021(4)	1.3(1)
N	0.1716(3)	0.2027(3)	0.3235(4)	1.6(1)
O(W)	0.0	0.4343(4)	0.25	3.9(2)

*$B_{eq} = \frac{4}{3}\sum_{ij}(a_i a_j)B_{ij}$ (16).

TABLE 5. Relevant interatomic bond distances (Å) and angles (deg) for coordination around copper atom and the TRIS group

Atoms	Distance
Cu—O(1)	1.958(2)
Cu—N	2.028(4)
Cu—O(W)	2.189(4)
C(1)—O(1)	1.416(6)
C(1)—C(4)	1.530(6)
C(2)—O(2)	1.419(5)
C(2)—C(4)	1.524(6)
C(3)—O(3)	1.414(5)
C(3)—C(4)	1.530(5)
C(4)—N	1.488(5)

Bonds	Angle
O(1)—Cu—N	84.5(1)
O(1)—Cu—O(W)	94.3(1)
N—Cu—O(W)	98.8(1)
O(1)—C(1)—C(4)	111.2(3)
O(2)—C(2)—C(4)	112.1(3)
O(3)—C(3)—C(4)	110.4(3)
C(1)—C(4)—C(2)	111.5(3)
C(1)—C(4)—C(3)	111.4(3)
C(1)—C(4)—N	105.0(3)
C(2)—C(4)—C(3)	110.6(3)
C(2)—C(4)—N	111.6(3)
C(3)—C(4)—N	106.5(3)

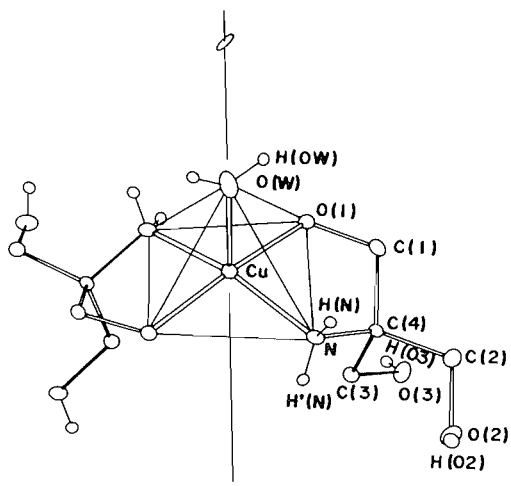

FIG. 9. Projection of the coordination around the copper atom. The atoms not named are related to the named atoms through a two-fold axis.

the same two-fold axis. Five atoms coordinate the copper atom forming an approximate pyramid with a rectangular basis as depicted in Fig. 9, which has its base formed by a pair of oxygen and nitrogen atoms. The atoms of each pair are related by a two-fold axis and belong to two symmetrically related tris(hydroxymethyl)aminomethane groups. The vertex of the pyramid is formed by the oxygen atom located on the two-fold axis. In a unit cell there are four coordination complexes linked to one another by a system of hydrogen bonds (Fig. 10).

Discussion

The formation curves were obtained on the basis of the

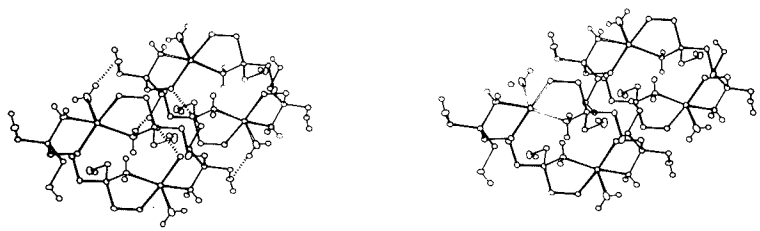

FIG. 10. Projection of the molecular packing showing the interaction through hydrogen bonds between four groups of the type depicted in Fig. 9.

TABLE 6. Relevant distances (Å) and angles (deg) in hydrogen bonds

Atoms	Distance O...O	Distance H...O	Angle O—H...O
O(3)—H(03)...O(1)	2.585(4)	0.72(4)	165.(1)
O(2)—H(02)...O(1)	2.716(4)	0.67(4)	175.(1)
O(W)—H(0W)...O(2)	2.752(4)	0.75(4)	162.(1)
N—H(N)...O(3)	3.113(5)	0.79(3)	168.(1)

equilibrium constants and reaction steps proposed for the Cu^{2+}—TRIS system (10).

The equilibrium analysis is rather complicated since eight different species are present in solution. Three species will be very predominant at different pH values: (*1*) the chelate complex $M(H_{-1}L)_2$ which above pH 9.5 is the only species present in solution; (*2*) the species ML_4 which near pH 7.6 is predominant and (*3*) the free solvated copper ion below pH 4.0. Together with the epr data, this analysis suggests that the highest pH complex observed by epr (complex **1**) could be assigned to the chelate since two nitrogen ligands show themselves in the room temperature spectrum. Our epr data show that the presence of this complex is significant down to pH 7.6 while the formation curves predict that at this low pH only ML_4 species would be significant. Therefore, our epr data seem to indicate that the formation curves in the region of pH above 7.2 should be displaced to lower pH, so that at pH 7.6 approximately 50% of the chelate species is present in the solution. This would require values for K_4 and K_{2b} to be lower and higher, respectively, than those given in ref. 10. Martell (10) considered the complete deprotonation of the hydroxyl groups, this leading to the structure corresponding to an uncharged species $M(H_{-1}L)_2$. This structure is essentially the same as the one obtained from X-ray crystallography except for the water molecule (see Fig. 9).

The epr results with the frozen solution suggest the occurrence of a rhombic distortion which is also observed for the high pH complex in the single crystal.

With regard to the optical spectra obtained at high pH it should be mentioned that similar complexes of aminoacids, where nitrogen and oxygen (carboxylate) ligands are involved, usually show a single broad band. In our case the splitting of the optical band is quite unusual; this could be explained alternatively in one of the following ways: (*a*) at high pH there is a coexistence of two different species, which have exactly the same epr spectrum, namely, $M(H_{-1}L)_2$ and $M(H_{-1}LL)^+$; the two optical bands are due to these different species and the formation curve for complex $(MH_{-1}LL)^+$ is wrong. (*b*) At high pH there is a single species with an optical band split in two bands. We believe this hypothesis should be preferred because upon freezing the splitting in the epr spectrum is not observed. Also, it is in closer agreement with the formation curves.

In the pH range between 6.0 and 7.5 the species which is predominant corresponds to our complex **2**. The equilibrium constant K_4 has to be corrected so that its maximum intensity would be shifted to pH 6.7 as indicated by the optical data (Fig. 4*a*).

Acknowledgements

We thank the Brazilian Agencies CNPq, FINEP, CAPES for partial financial support through research grants. We also appreciate the effective assistance from Mr. Valdeci Massaro for computer spectral analysis.

1. H. C. FREEMAN. *In* Inorganic biochemistry. *Edited by* G. I. Eichorn. Elsevier, Amsterdam. 1973. Chap. 4.
2. J. F. BOAS, J. R. PILBROW, and T. D. SMITH. Biological magnetic resonance. *Edited by* L. J. Berliner and J. Reuben. Plenum Press. 1978.
3. D. J. E. INGRAM. Biological and biochemical applications of ESR. Adam Hilger Ltd., London. 1969.
4. B. J. HATHAWAY and B. E. BILLING. Coordin. Chem. Rev. **5**, 143 (1970).
5. L. SPORTELLI, H. NEUBACHER, and W. LOHMANN. Biophys. Struct. Mechanism. **3**, 317 (1977).
6. H. KOZLOWSKI and B. J. TREZEBIATOWSKA. J. Mol. Struct. **45**, 159 (1978).
7. O. R. NASCIMENTO and M. TABAK. J. Inorg. Biochem. **23**, 13 (1985).
8. S. HARKEMA, J. W. BATS, A. M. WEYENBERG, and D. FEIL. Acta Crystallogr. B**29**, 143 (1973).
9. R. RUDMAN, D. EHNERMAN, and S. J. LA PLACE. Science, **200**, 531 (1978).
10. K. S. BAI and A. F. MARTELL. J. Inorg. Nucl. Chem. **31**, 1697 (1969).
11. D. T. CROMER and J. B. MANN. Acta Crystallogr. **24**, 321 (1968).
12. D. T. CROMER and D. LIBERMAN. J. Chem. Phys. **53**, 1891 (1970).
13. R. F. STEWART, E. R. DAVIDSON, and W. T. SIMPSON. J. Chem. Phys. **42**, 3175 (1965).
14. G. M. SHELDRICK. SHELX-76 program for crystal structure determination. University of Cambridge. 1976.
15. C. K. JOHNSON. ORTEP. Report ORNL-3794, Oak Ridge National Laboratory, TN. 1965.
16. W. C. HAMILTON. Acta Crystallogr. **12**, 609 (1959).